

# IMPEDANCE AND THERMAL STUDIES OF THE CERN SPS WIRE SCANNERS AND MITIGATION OF WIRE HEATING

E. de la Fuente <sup>\*</sup>, I. Papazoglou, L. Sito <sup>†</sup>, W. Andreazza, C. Antuono, N. Bruchon, R. Calaga, F. Carra, J. Emery, A. Harrison, I. Karpov, K. Li, G. Papotti, F. Roncarolo, G. Rumolo, B. Salvant, M. Sullivan, R. Veness, A. Vanel, C. Vollinger, and C. Zannini  
European Organization for Nuclear Research (CERN), Geneva, Switzerland

## Abstract

All wires of the four CERN SPS rotational wire scanners failed when increasing the beam intensity towards the target for the LHC Injector Upgrade in 2023. Impedance and thermal studies were immediately launched, with simulations and measurements indicating that beam-induced heating from resonant modes on the thin wire could be sufficient to cause these breakages. Mitigation measures to displace electromagnetic losses away from the wire were proposed and implemented. This allowed a much higher beam intensity to be reached, close to the LIU target. Simulations now predict that the modified wire scanners can sustain the LIU beam parameters.

## INTRODUCTION

Beam wire scanners (BWS) are crucial tools in accelerator physics for measuring the transverse profile of particle beams. In the CERN SPS, the four rotating BWS units are regularly used to optimize beam emittance and estimate beam tail population [1]. However, these devices face challenges due to the intense thermal loads experienced by the carbon wire during high-intensity runs. Wire breakages have been observed both while scanning the beam and in parking position. These breakages were explained in the past by electromagnetic coupling with the wire when the beam intensity and bunch length were pushed. The mitigation measures consisted in changing the wire material [2] and in the addition of ferrite slabs inside the BWS tank [3].

On the 12th of April 2023, during the scrubbing run, an incident highlighted the susceptibility of the wires in the new BWS, with all four wires found broken when in parking position, coinciding with the acceleration of unprecedented beam intensities in the SPS. Consequently, two out of four wires were exchanged, only to break again on the 22nd of April, this time with 10% lower beam intensities on a standard LHC filling cycle [4].

In the following sections, we detail the methodology employed to investigate whether beam-induced heating could have been the cause of wire breakages. The beam-coupling impedance simulations and beam-induced power calculations will be discussed, together with a thermal analysis of the structure. Subsequently, by adopting this methodology, it was possible to perform a quantitative analysis of several mitigation strategies. The optimal solution will be presented.

<sup>\*</sup> elena.de.la.fuente.garcia@cern.ch

<sup>†</sup> leonardo.sito@cern.ch

## BEAM-INDUCED HEATING STUDIES

When reaching high intensities with small bunch lengths, beam-induced heating (BIH) could severely damage accelerator components [5]. This effect is caused by electromagnetic coupling between the beam of charged particles and the surrounding environment (i.e. the accelerator device itself). Typically, this interaction is described in the frequency domain introducing a complex vector quantity called beam-coupling impedance [6, 7], which is a characteristic quantity of the device geometry and material.

The beam-coupling impedance allows for a convenient quantification of the power lost by the beam, and thus deposited on the accelerator device [8, 9]:

$$P = 2(f_0 e N_{beam})^2 \cdot \sum_{p=0}^{+\infty} |\Lambda(p\omega_0)|^2 \Re(Z_z(p\omega_0)), \quad (1)$$

where  $f_0$  is the revolution frequency of the machine,  $e$  is the charge of the beam particle,  $N_{beam}$  is the number of particles in the beam,  $\Lambda$  is the normalized beam spectrum (i.e. the Fourier-transform of the beam charge distribution),  $\Re(Z_z)$  is the real part of the longitudinal component of the beam-coupling impedance.

### Breakage Scenario

In order to determine the cause of the breakage, the beam-induced power dissipated in the device was computed assuming the beam parameters at the time of the second breakage (22nd of April):

- four trains of 72 bunches with a measured average intensity per bunch of  $1.8 \times 10^{11}$  ppb,
- the mean bunch length spanned from 3.5 ns at injection to 1.6 ns at top energy.

The beam-coupling impedance of the device was obtained through full-wave electromagnetic simulations performed with CST wakefield solver [10]. The impedance curve obtained is shown in Fig. 1 on the right vertical axis (black curve). It is possible to appreciate the presence of a peak overlapping the normalized beam spectrum close to 800 MHz. This is particularly detrimental since it couples with the carbon wire as seen in the field maps of the modes resonating in the device. At this point, the power loss computation was performed using the python package `bihc` [11, 12] which implements Eq. 1 and allows a more sophisticated analysis that will be discussed in detail in the following part.

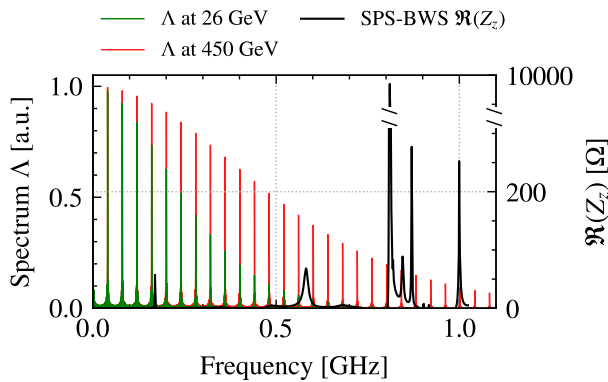


Figure 1: Normalized beam spectrum ( $\Lambda$ ) at injection and flat top (left axis). Real part of the longitudinal impedance in the breakage scenario (right axis).

One crucial point in this study was also understanding the impact of the time evolution of the bunch length during the cycle on the power dissipated on the wire: a lower bunch length will result in a beam spectrum extending to higher frequencies. This is shown in Fig. 1 where the spectrum is reported on the left vertical axis at injection (26 GeV) and top energy (450 GeV). Since the total power loss is given by a weighted sum (Eq. (1)), higher frequency terms of the impedance curve will make a larger impact with a shorter bunch length.

To properly account for the time evolution of the bunch length, several measurements were performed to obtain the longitudinal beam charge profile along the energy ramp. This allowed to compute the power loss as a function of time. Finally, combining the CST simulation results and the total power loss obtained with `bihc`, it was possible to extract the power deposited on the wire, again as a function of time during the cycle.

However, in the case of impedance curves with several modes or peaks (as for the BWS), the power loss computation is highly sensitive to the peak frequency. More specifically, if the impedance peak overlaps with one of the beam's spectral lines, the power loss contribution will significantly rise. The frequency of the peaks in an impedance curve (obtained from simulations or measurements) has some inherent uncertainty. To account for this, `bihc` [11] can perform a statistical analysis: the considered impedance curve, gets shifted rigidly in frequency, within  $\pm 40$  MHz, in steps of  $f_0$ . In this way it is possible to get an average, minimum and maximum power loss estimation, reported on the left plot of Fig. 2. Moreover, the statistical occurrence of the power loss values computed when applying the frequency shift can be obtained. This is shown, for the last time step (top energy), on the right side of Fig. 2.

The BIH power is assumed to be uniformly distributed along the mass of the wire. The problem of the wire heating and cooling was modelled analytically following [13] with some simplifications: i) the conductive cooling at the edges of the wire is neglected due to the small cross-section of the

wire and ii) the sublimation of the wire is not considered as this phenomenon occurs when the wire fails. This means that two cooling mechanisms are dominant: radiative cooling, driven by the Stephan-Boltzmann law and thermionic emission, driven by the Richardson-Dushman equation. Moreover, a dynamic calculation is implemented following the BIH power loss time profile. This is due to the wire's low volume over external surface ratio, low mass and high reached temperatures, which cause the wire to heat up and cool down in milliseconds. The maximum temperature calculated for the wire is 3540 K assuming the maximum power loss curve and 1855 K assuming the minimum power loss curve. As the broken wire showed signs of sublimation, the temperatures reached values closer to the worst-case scenario.

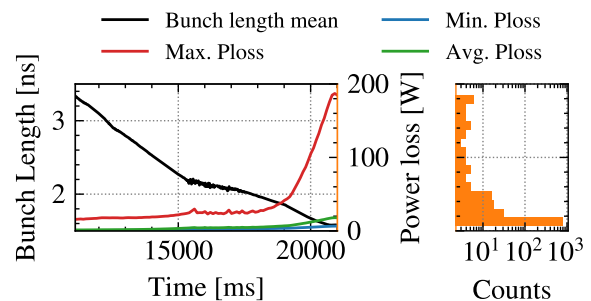


Figure 2: Evolution along the ramp of the power loss on the wire (second y-axis) for the breakage scenario. The bunch length evolution is reported on the first y-axis. A histogram reporting the probability of having a certain dissipated power value, for the last time step of the computation, is shown on the right side.

### Mitigations Implemented in 2023

A study campaign was launched to find a possible solution to the excessive heating of the carbon wire due to BIH. The methodology was the same adopted for the breakage scenario but the beam intensity employed for the calculations was  $2.3 \times 10^{11}$  ppb. This allowed finding a mitigation option which would also guarantee compliance with LIU requirements [14].

The mitigation solutions focused on reducing the electromagnetic coupling between the beam and the wire. As already shown in the past [2], adding ferrite tiles inside the BWS tank helps reduce the EM power deposited on the wire concentrating the magnetic field into the ferrite material.

Simulations of different ferrite tile installations were carried out, and 2023 operation confirmed that an optimal mitigation solution consists of a combination of inserting five ferrite tiles in the tank together with the installation of a radiofrequency (RF) rod coupler. The RF coupler consists of a capacitively coupled rod installed via a ceramic feed-through and protruding into the BWS shaft (see [15] for details). It was demonstrated that this coupler allows taking out a significant amount of power from the BWS tank. In addition, the RF rod coupler provides the possibility to record the beam-induced power spectrum and will help to

detect potential wire breakage hazards in the future. This combined solution allows having: a) minimal modifications of the existing structure, b) drastic reduction of the power going to the wire, and c) a relatively low power dissipated on each ferrite tile. In this way, the tiles are not heating excessively thus preventing significant outgassing levels. A 3D CAD model of this mitigation option is shown in Fig. 3.

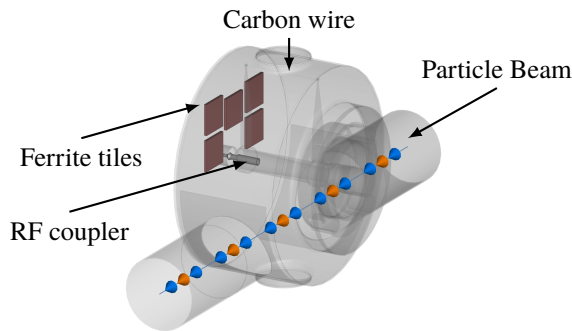


Figure 3: 3D CAD model of the SPS beam wire scanners and the mitigation solutions implemented.

The effects of the mitigation strategy can be appreciated by looking at the impedance curve (Fig. 4). Here a comparison of the impedance before and after the mitigation is shown. The peaks are significantly lower and broadened in frequency.

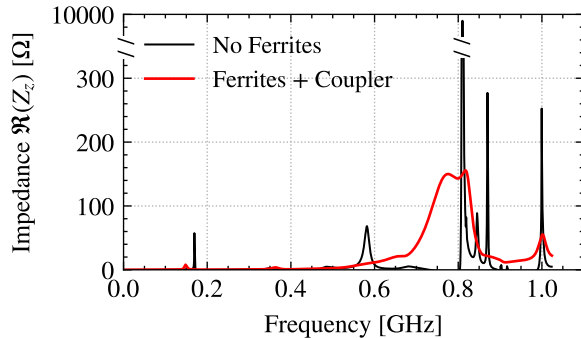


Figure 4: Comparison of the real part of the longitudinal impedance before and after the mitigation.

This significantly decreases the maximum power loss, which is now below the minimum dissipated power of the breakage scenario. Moreover, the broader impedance peaks will result in a lower spreading of the power loss value between the maximum, minimum and average cases. The power dissipated on the wire as a function of time is reported in Fig. 5. Under these conditions, the wire is expected to reach maximum temperatures between 1600 K and 1725 K. For estimating the temperature reached by the BWS tank and the included ferrite tiles, an ANSYS model was employed. From electromagnetic and BIH simulations, the total power going to the ferrites was extracted and used as input. For this scenario, a steady state analysis considering an average power over the cycle was used. This is reasonable since, in

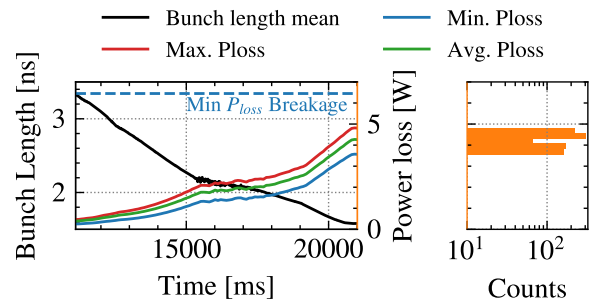


Figure 5: Power loss on the wire evolution along the ramp (second y-axis) for the mitigation solution. The dashed line is the minimum power loss value of the breakage scenario.

the case of the ferrites, their volume is large compared to their external surface. This means that, contrary to the wire case, they require several minutes to reach maximum temperature. In the worst-case scenario, the maximum temperature for the ferrites tiles resulted in 45.7 °C and in 25.2 °C for the tank. In Fig. 6 the temperature map obtained from ANSYS is shown.

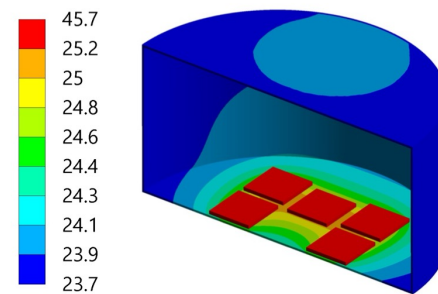


Figure 6: Temperature map of the ferrite tiles and BWS tank heating in the mitigation scenario. Values reported in °C.

## CONCLUSION

The methodology employed for the study of the 2023 BWS wires' breakage was shown along with the most significant results. Combined electromagnetic and thermal simulations allowed to quantitatively assess the breakage condition (in terms of power dissipated and temperature reached by the wire before sublimation). The best mitigation option significantly reduced the power on the wire, leading to wire temperatures that now look comfortable for operation with LIU target parameters. Moreover, the expected temperature of the ferrite tiles does not indicate risks of outgassing. The mitigation solution was installed in July 2023 to be tested during operation before the end-of-the-year technical stop and finally implemented in all the SPS wire scanners during the end-of-year technical stop. During the 2024 scrubbing run, LIU intensities with nominal bunch length were achieved for the first time in the SPS. The BWS was closely monitored and the wire showed smooth voltage and temperature signals confirming experimentally the validity of the impedance mitigation solution.

## REFERENCES

- [1] F. Asvesta *et al.*, “Characterization of transverse profiles along the LHC injector chain at CERN”, in *Proc. IPAC’23*, Venice, Italy, 2023, pp. 3490–3493, doi:10.18429/JACoW-IPAC2023-WEPL158
- [2] F. Roncarolo *et al.*, “Cavity Mode Related Wire Breaking of the SPS Wire Scanners and Loss Measurements of Wire Materials”, in *Proc. PAC’03*, Portland, OR, USA, May 2003, pp. 2470–2472, <https://jacow.org/p03/papers/WPPB026.pdf>
- [3] E. Piselli *et al.*, “CERN-SPS Wire Scanner Impedance and Wire Heating Studies”, in *Proc. IBIC’14*, Monterey, CA, USA, Sep. 2014, pp. 88–92, <https://jacow.org/IBIC2014/papers/MOPF16.pdf>
- [4] R. Veness *et al.*, “Overview of beam intensity issues and mitigations in the CERN-SPS fast wire scanners”, presented at IPAC’24, Nashville, TN, USA, May 2024, paper WEPG26, this conference.
- [5] B. Salvant *et al.*, “Beam Induced RF Heating in LHC in 2015”, in *Proc. IPAC’16*, Busan, Korea, 2016, pp. 602–605, doi:10.18429/JACoW-IPAC2016-MOPOR008
- [6] A. W. Chao, *Physics of collective beam instabilities in high energy accelerators*. Wiley, 1993.
- [7] L. Palumbo, V. G. Vaccaro, and M. Zobov, *Wake fields and impedance*, Lecture given at the ‘CAS Advanced School on Accelerator Physics’ Rhodes - Greece 20 Sept. 1 Oct. (1994), 1994, doi:10.15161/oar.it/1448441728.46
- [8] C. Zannini, G. Iadarola, and G. Rumolo, “Power Loss Calculation in Separated and Common Beam Chambers of the LHC”, in *Proc. IPAC’14*, Dresden, Germany, Jun. 2014, pp. 1711–1713, doi:10.18429/JACoW-IPAC2014-TUPRI061
- [9] F. Fienga *et al.*, “Direct measurement of beam-induced heating on accelerator pipes with fiber optic sensors: Numerical analysis validation”, *IEEE Transactions on Instrumentation and Measurement*, vol. 72, pp. 1–9, 2023, doi:10.1109/TIM.2023.3279420
- [10] Computer Simulation Technology, *CST Studio Suite*, <https://www.cst.com/products/cstsuite>.
- [11] E. de la Fuente Garcia, F. Giordano, B. Salvant, L. Sito, and C. Zannini, *bihc, a python tool for beam induced heating computations*, <https://github.com/ImpedanCEI/BIHC>.
- [12] L. Sito *et al.*, “A Python Package to Compute Beam-Induced Heating in Particle Accelerators and Applications”, in *Proc. 68th Adv. Beam Dyn. Workshop High-Intensity High-Brightness Hadron Beams (HB’23)*, Geneva, Switzerland, Oct. 9–13, 2023, 2024, pp. 611–614, doi:10.18429/JACoW-HB2023-THBP52
- [13] M. Sapinski, “Model of Carbon Wire Heating in Accelerator Beam”, CERN, Tech. Rep., 2008, <https://cds.cern.ch/record/1123363>
- [14] G. Rumolo *et al.*, “Beam Performance with the LHC Injectors Upgrade”, in *Proc. 68th Adv. Beam Dyn. Workshop High-Intensity High-Brightness Hadron Beams (HB’23)*, Geneva, Switzerland, Oct. 9–13, 2023, 2024, pp. 1–8, doi:10.18429/JACoW-HB2023-MOA1I1
- [15] C. Vollinger, M. Sullivan, and M. Neroni, “Mitigation of beam coupling impedance for the wire scanners in the CERN Super Proton Synchrotron”, presented at IPAC’24, Nashville, TN, USA, May 2024, paper THPC51, this conference.